Behavior of Self Compacted Concrete Deep Beams Reinforced With Polypropylene Fibers

Ata El-kareim Shoeib[1]**, Mohamed Said**[2]**, Amal Hassanin**[1]**, Mohamed Said Badawy**[*1]

[1] Department of civil Engineering , Faculty of Engineering Helwan University, Cairo, Egypt .

[2] Department of civil Engineering , Faculty of Engineering at Shoubra, Benha University, Cairo, Egypt .

* Corresponding author.

E-mail:mohamedsaid3644@gmail.com,dramalh@yahoo.com,atta_alasayed@m-eng.helwan.edu.eg,

Mohamed.abdelghaffar@feng.bu.edu.eg.

Abstract: Self-compacting concrete (SCC) is one of the most recent high-performance concrete innovations. The behavior of self-compacted concrete deep beams reinforced with polypropylene fibers herein investigated. Within an experimental program comprising thirteen simply supported beams tested to failure. The parameters in perspective are polypropylene fiber ratios (0.0, 0.30, 0.60, and 0.90 %), vertical web reinforcement, and horizontal web reinforcement. Mid-span deflection, cracks, and strains are measured for each specimen. According to the test results, the polypropylene fibers improved the cracking load, ultimate capacity, displacement, and energy absorption of the tested SCC deep beams. A polypropylene fiber content of 0.90 % resulted in the most significant improvement as regards the performance of deep beams. The improvement in ultimate capacity reached a 30% magnitude compared to specimen B1. Test results showed that both vertical and horizontal web reinforcement are effective in enhancing the shear capacity of SCC deep beams. The test results were compared with the ACI design method to show the impact of web reinforcement ratio on deep beam load capacity.

Keywords: Deep beams, polypropylene fibers, Self-compacting concrete, Web Reinforcement.

1. INTRODUCTION

ACI 318-19 [1] defines a deep beam as a structural member having a clear span no more than four times the overall depth or with concentrated loads applied at a distance no greater than two times the depth from the face of the support. When removing a lower column from a structure, a deep beam or transfer girder is used. To transmit the strong axial forces of the columns above to the supporting columns below, it is occasionally necessary to use the complete depth of the floor-to-floor height [2–4].

Deep beams are typically narrow in width and contain congested shear reinforcement. Therefore, during pouring, traditional concrete does not flow well and does not fill the bottom portion fully. This results in several problems with the concrete, including voids, segregation, poor bonding with reinforcing bars, and surface holes. So, SCC is an ideal casting material for these members. Due to its liquid nature, self-compacting concrete offers distinct advantages over traditional vibrated concrete, such as elimination of the issues mentioned above, low level of noise in construction, faster building, and improvement in quality and durability, as well as no need for vibration where it can fill all spaces in the formwork and moves by its weight

through reinforcing bars [5–7]. Okamura was the first to develop self-compacting concrete (SCC) in 1986 [8]. Several significant studies have been published on the structural shear behavior and performance of RC structures built using SCC [9–13].

Increasing the percentages of horizontal and vertical grids or integrating or partly replacing shear reinforcements with fiber-reinforced concrete (FRC) boosts the strength and decreases the brittleness of deep beams [14–17]. For centuries, short fibers have been used to strengthen fragile materials such as cement and concrete composites. Steel, glass, synthetic materials, and some natural fibers are among the many fiber kinds now available for commercial application [18]. Polypropylene fiber (PP fiber) is often utilized in cement and concrete composites to increase the toughness and ductility of the matrix composite owing to its low modulus of elasticity, high strength, outstanding ductility, significant durability performance, and cost-effectiveness [19]. An abundance of earlier research efforts used various PP fiber percentages to investigate the influence of this fiber on a variety of parameters [20–26].

Experimentally studying the behavior of self-compacted concrete deep beams with and without Polypropylene

Fibers is the main objective of this paper. The fundamental purpose herein is to explore the impacts of the factors included in this analysis, such as the content of Polypropylene fibers, (Vpp), and the vertical and horizontal transverse reinforcement ratios

2. EXPERIMENTAL PROGRAM

2.1. Test specimens

The experimental program consisted of thirteen deep beams with simple support. All beams were constructed in the reinforced concrete laboratory of Helwan University's El-Mataria Faculty of Engineering. All beams had dimensions of 650 mm in depth, 120 mm in width, and 1200 mm in length. The reinforcement and concrete dimensions of beams are depicted in Fig. 1. The details of all tested deep beams are shown in Table 1.

Table 1. Details of tested beams

Group	Beam No.	Bottom longitudinal steel	Top longitudinal steel	V_{PP} %	Vertical Stirrups	Horizontal Stirrups
G1	B1	4φ18	2φ12	0	-	-
	B2	4φ18	2φ12	0.3	-	-
	B3	4φ18	2φ12	0.6	-	-
	B4	4φ18	2φ12	0.9	-	-
G2	B5	4φ18	2φ12	0.6	φ8 / 200	-
	B6	4φ18	2φ12	0.6	φ8 / 150	-
	B7	4φ18	2φ12	0.6	φ8 / 100	-
G3	B8	4φ18	2φ12	0.6	-	φ8 / 200
	B9	4φ18	2φ12	0.6	-	φ8 / 150
	B10	4φ18	2φ12	0.6	-	φ8 / 100
G4	B11	4φ18	2φ12	0.6	φ8 / 200	φ8 / 200
	B12	4φ18	2φ12	0.6	φ8 / 150	φ8 / 150
	B13	4φ18	2φ12	0.6	φ8 / 100	φ8 / 100

2.2. Materials

The materials used to cast the specimens are coarse aggregate, natural clean sand, Ordinary Portland cement, potable water, polypropylene fiber, Silica fume, and a superplasticizer. Table 2 displays the proportions of the concrete mixture utilized in this study. Cementitious materials consist of Ordinary Portland Cement of the type CEM I 42.5 N and Silica Fume. The coarse aggregate was natural dolomite with a maximum nominal size of 10 mm. Master Glenium RMC 315 from BASF Company was used

as the super-plasticizer in all of the mixes. Master Fiber 249 was used as the polypropylene fiber. The length of fiber was 48mm. The diameter was 0.85mm and the Modulus of elasticity was 4.7 GPa. In the experimental tests, two types of reinforcing steel were utilized. The first material utilized as vertical and horizontal shear reinforcement was mild steel (grade 24/35). The second type, grade 40/60 high-tensile steel, was used for the main bottom and top reinforcement. During the pouring of deep beams, three 150×150×150 mm cubes were taken from each mix to measure the concrete's strength.
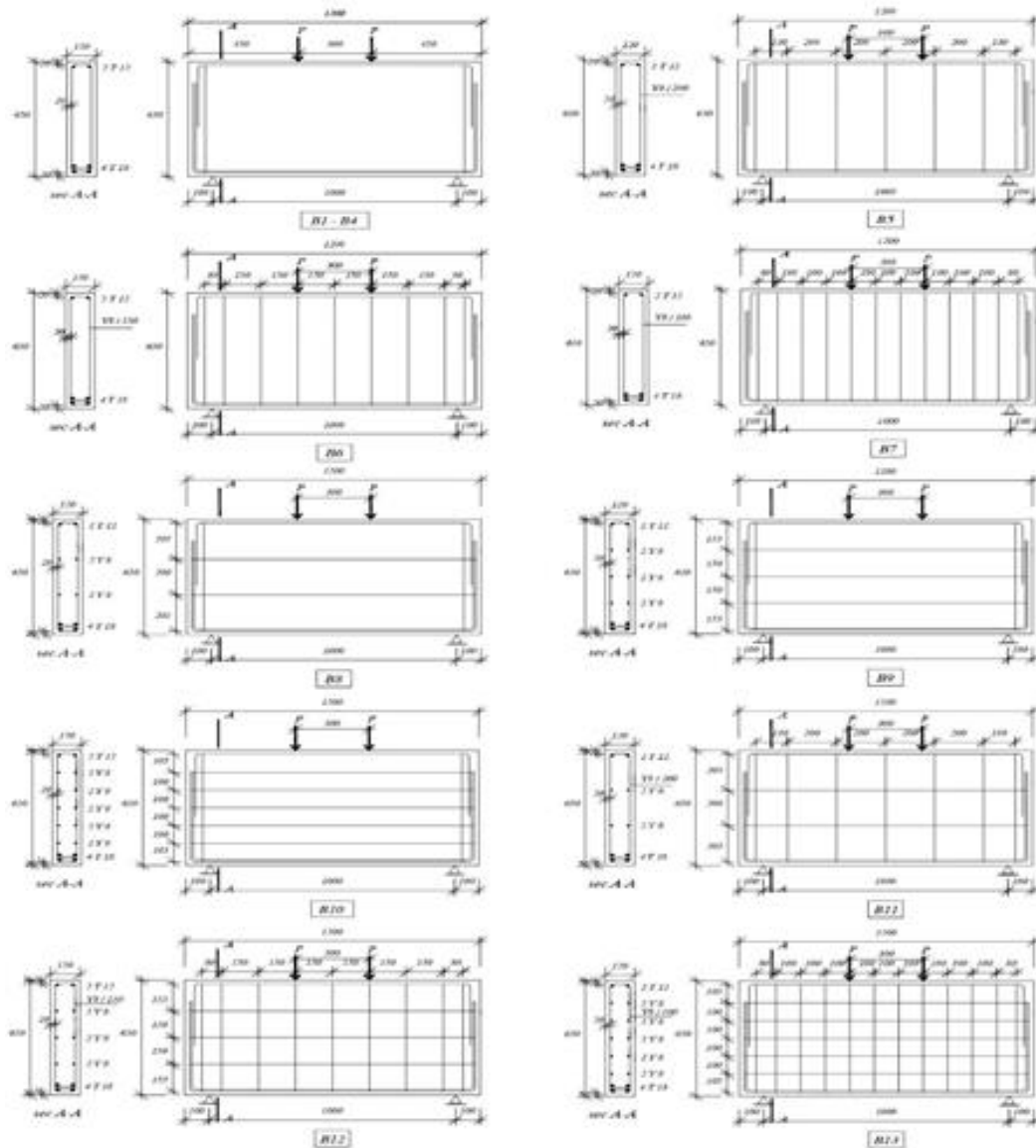
Fig 1. Details of beams

Table 2. proportions of the concrete mix

Mix No.	(kg / m3)					%	
	cement	sand	Dolomite	Silica Fume	Water	V_{pp}	Super Plasticizer
1	495	870	780	55	192.5	0	1.5
2	495	870	780	55	192.5	0.3	2.1
3	495	870	780	55	192.5	0.6	2.7
4	495	870	780	55	192.5	0.9	3.3

2.3. Tests on self-compacting concrete

As depicted in Figs. 2 and 3, the slump flow test, the T50 cm slump flow test, and the L-box were used to evaluate the material properties of fresh concrete. Table 3 displays the results of fresh Self Compacting Concrete property tests. These results meet the criteria for SCC as established by ACI committee-363 [27].

Fig 2. Concrete measurement diameter

Figure 3. L- Box test setup

Table 3. proportions of the concrete mix

Mix No.	Slump flow (mm)	T50 (sec)	L-Box (H2/H1)
1	660	4	0.85
2	730	3	0.93
3	750	2.5	0.96
4	710	3.5	0.89
Limit ACI - 363	650 – 800	2 - 5	0.8 - 1

A compression test for standard cubes was used to measure the concrete strength of test specimens at the time of testing. Table 4 displays the results of the cube strength test.

Table 4. The cube strength test results

Cube No	Mix (1)	Mix (2)	Mix (3)	Mix (4)
F_{cu} (Mpa)	47	52	60	64

2.4. Instrumentation and test procedure

On test specimens, the applied load, deflection, bottom reinforcement strain, and vertical and horizontal stirrup strains were measured. The deflection of the tested concrete deep beams was monitored using linear variable differential transducers (LVDTs). During testing, the deep beam's deflection was measured with LVDTs. Two LVDTs were placed between the point of loading, support from the left and right sides of the deep beam, and one LVDT was placed in the middle of the deep beam. All of the LVDTs were attached to the bottom of the deep beam. Fig. 4 depicts a typical test setup for tested specimens. The LVDT, load cell, and strain gauge measurements are acquired automatically and shown on a digital display device. During the test, the crack developed on the deep beam surface were noted and documented till failure.

Fig 4. Test Setup

3. TEST RESULTS

3.1. Crack of pattern and mode of failure

Fig. 5 depicts the typical behavior of beams. crack pattern distributions recorded at applied load increments. All of the tested beams behaved elastically at low load levels, with no defects in their structure or cracks appearing anywhere, and midspan deflections that are small and proportional to the applied load. In general, The first flexure crack is noticed in the beam's lower part between load locations at a loading level ranging from 31% to 38% of the ultimate load. The first diagonal crack develops in the middle third of the load- and support-bounded diagonal zone. As the load increases, the inclined cracks enlarge and extend toward the support and

load locations, and more parallel cracks develop near the support.

In deep beams, a substantial percentage of the load is transmitted directly to the support using compression struts placed between the load and the supporting points. This kind of load transmission results in the most common form of failure in deep beams. As depicted in Fig. 5, shear failure was detected in all specimens. Specimens B1 to B5 revealed a shear failure mechanism by cracking the web concrete along the line that connects the load pad and the beam support. The shear splitting failure occurred when the main crack formed and split the beam from top to bottom without crushing the concrete. Additional parallel diagonal cracks created a series of concrete struts in specimens that failed because of shear crushing. As shown in Fig. 5, one of the struts, containing horizontal stirrups only, failed due to diagonal shear crushing. Failure of beams B6 to B13 revealed the function of horizontal and vertical stirrups in changing the failure mechanism and raising the ultimate load.

3.2. Load-deflection relationship

The load-deflection responses of four different beam series are shown in Fig. 6. Deep beam deflections are generally small when compared to slender beams. The primary purpose of incorporating fibers into a cement matrix is to enhance the composite's crack and deformation resistance by boosting its tensile strength. As depicted in Fig. 6a, increasing the proportion of Polypropylene fibers improves the ultimate load-carrying capability of Polypropylene fiber reinforced concrete due to its increased post-cracking strength. The ultimate load of beams with no shear reinforcement was increased by 14%, 25%, and 30%, respectively, for specimens B2 with 0.30%, B3 with 0.60%, and B4 with 0.90% polypropylene fiber content, as shown in Table 5. As shown in Table 5, increasing the percentage of Polypropylene fibers from 0 to 0.9% increased the ultimate displacement from 3.60 mm to 5.22 mm.

Table 5. Test results

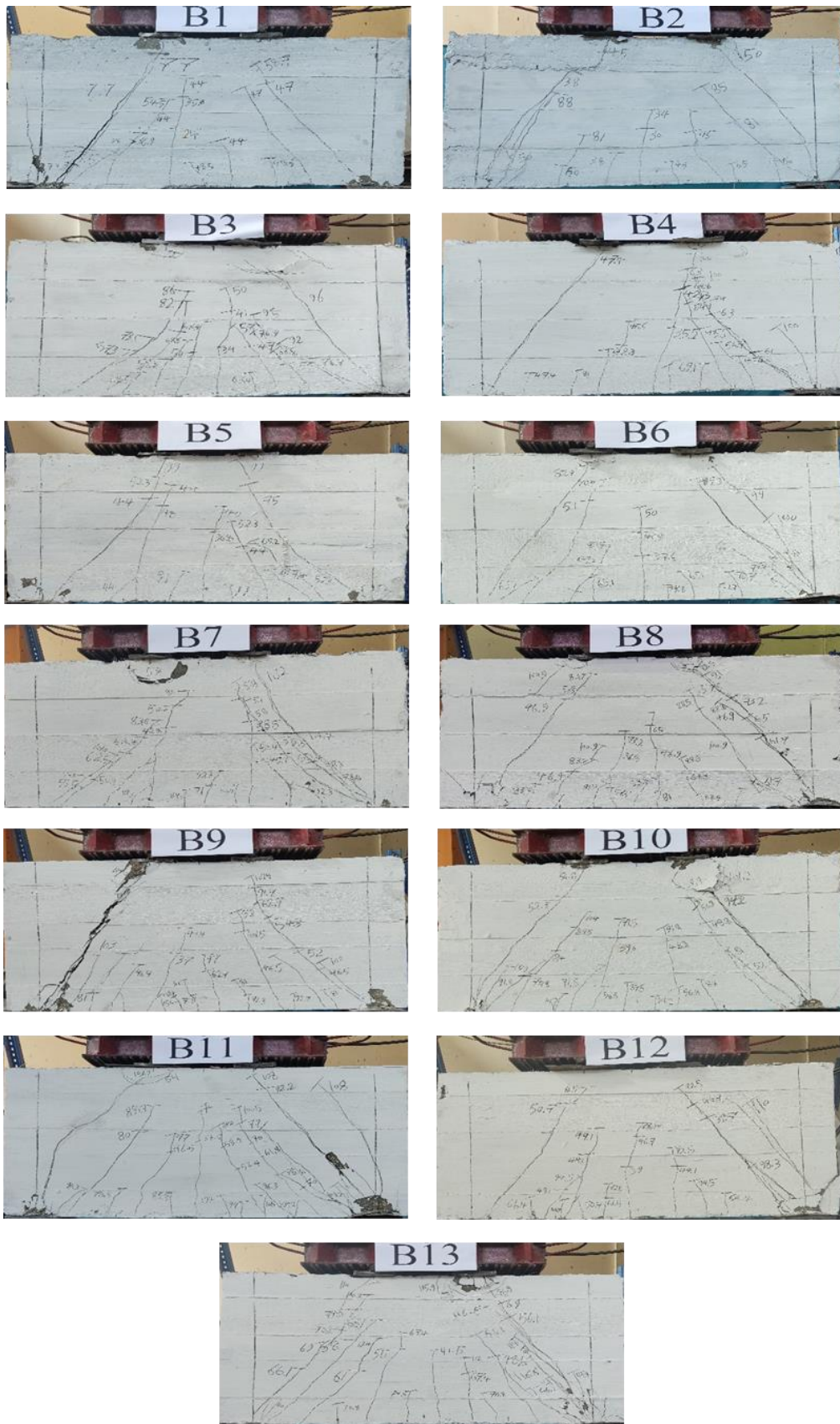| Beam No.	Δ_{cr} (mm)	P_{cr} (KN)	Δ_u (mm)	P_u (KN)	Absorbed energy (KN.mm)	Failure mode
B1	1.20	240	3.60	770	1411	Shear splitting
B2	1.56	300	4.50	880	2231	Shear splitting
B3	1.69	340	4.90	960	2618	Shear splitting
B4	1.79	352	5.22	1000	2939	Shear splitting
B5	1.80	368	5.25	990	2998	Shear splitting
B6	1.85	376	5.60	1000	3333	Shear crushing
B7	1.92	385	5.92	1020	3637	Shear crushing
B8	1.76	365	5.18	1009	2949	Shear crushing
B9	1.82	370	5.50	1030	3259	Shear splitting
B10	1.95	396	6.00	1090	3900	Shear crushing
B11	2.00	375	6.12	1080	3816	Shear crushing
B12	2.10	390	6.30	1100	4074	Shear crushing
B13	2.22	415	6.54	1165	4481	Shear crushing

Fig 5. Crack pattern and mode of failure
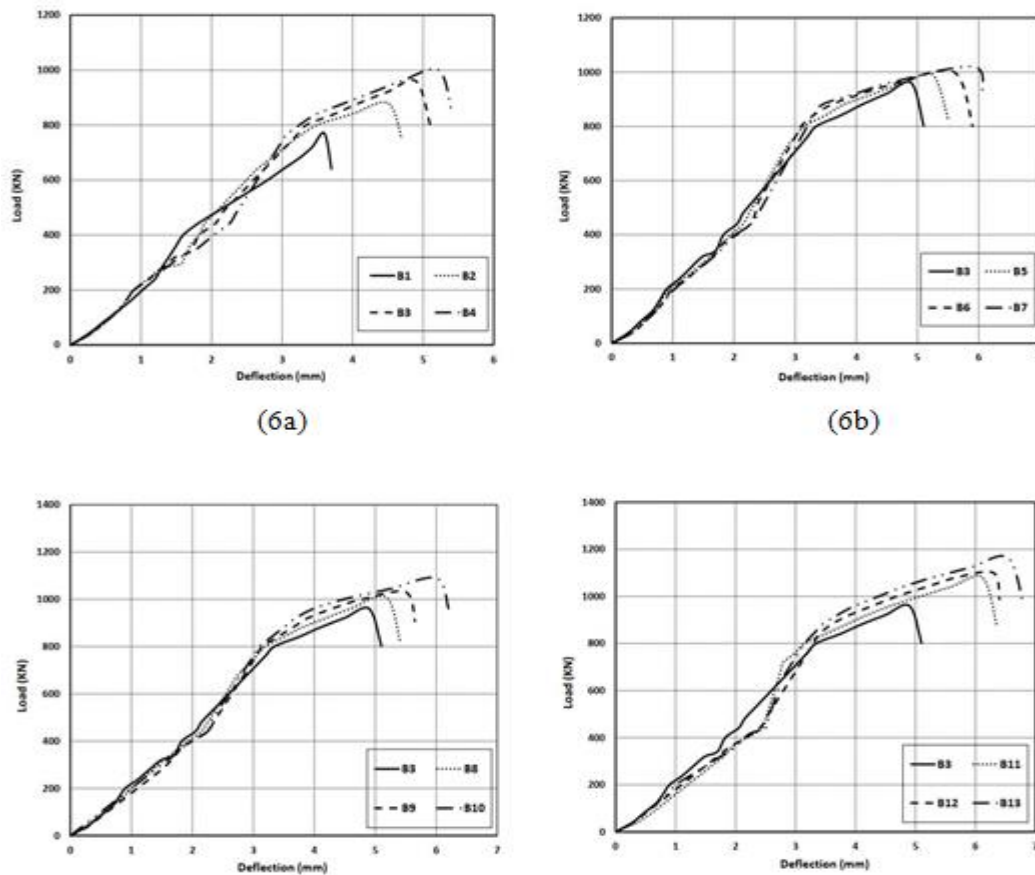
(6a)

(6b)

Fig 6. Load-deflection curve for tested beams

The load-displacement shown in Fig. 6b for specimens with a polypropylene fibers ratio of 0.6 percent and vertical reinforcement only, demonstrated that increasing the vertical stirrups content slightly increased the ultimate load. For specimen B7, the maximum increase in ultimate load was 6.25 %, while the maximum increase in ultimate displacement was 21%. Beam 10, on the other hand, with horizontal stirrups, demonstrated enhanced ultimate load and post-peak behavior. the maximum increase in ultimate load was 13.5%, while the maximum increase in ultimate displacement was 22.4%, as shown in Fig. 6c and table 5. Concerning the horizontal and vertical stirrups, significantly enhanced the ultimate load. For specimen B13, the maximum increase in ultimate load was 21.35 %, while the maximum increase in ultimate displacement was 33.5%, as shown in Fig. 6d.

3.3. Ductility

Failure due to brittleness severely affects the capacity and ductility of structural parts. The ability of specimens to disperse inelastic deformation energy is one of the most critical variables in determining their ductility. Mohammad Hassani et al. [28,29] determined that the total dissipated energy was equal to the sum of the areas contained by the

displacement. As depicted in Fig. 6, the dissipated energy grew as the level of displacement rose. Specimens reinforced with polypropylene fibers dissipated much more energy, as seen by the load-displacement zones contained by these specimens. The specimens strengthened with polypropylene fibers showed the greatest energy dissipation, as indicated in Table 5 and Fig. 7. The energy dissipation of specimens with polypropylene fibers increased by 58 %, 85.5 %, and 108 %, respectively, for specimens with 0.3 %, 0.6 %, and 0.9 % polypropylene fibers content compared with the control specimen containing no shear reinforcement. In addition, the ductility of the specimen increased as the spacing between horizontal and vertical stirrups reduced
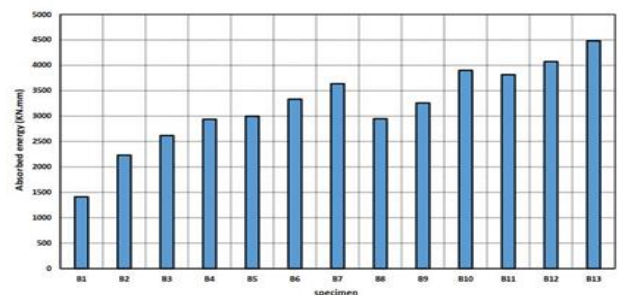

Fig 7. Absorbed energy of tested specimens

3.4. Strains in main reinforcement

To observe the variation of strain in flexural reinforcement, strain gauges were attached to the bottom steel bar of specimens. Fig. 8 depicts the load-strain relationship in the 18 mm-diameter primary reinforcing bar. A strain gauge is located in the center of the main bar. The relationship was linear until the first flexure crack in experimental deep beams. The strain values were eventually increased until they reached the failure load. The maximum strain in longitudinal tension bars was less than the yield value. All of the specimens' flexure modes of failure were secured, allowing for the shear mode of failure, as indicated by the measured strain in the bottom reinforcement.
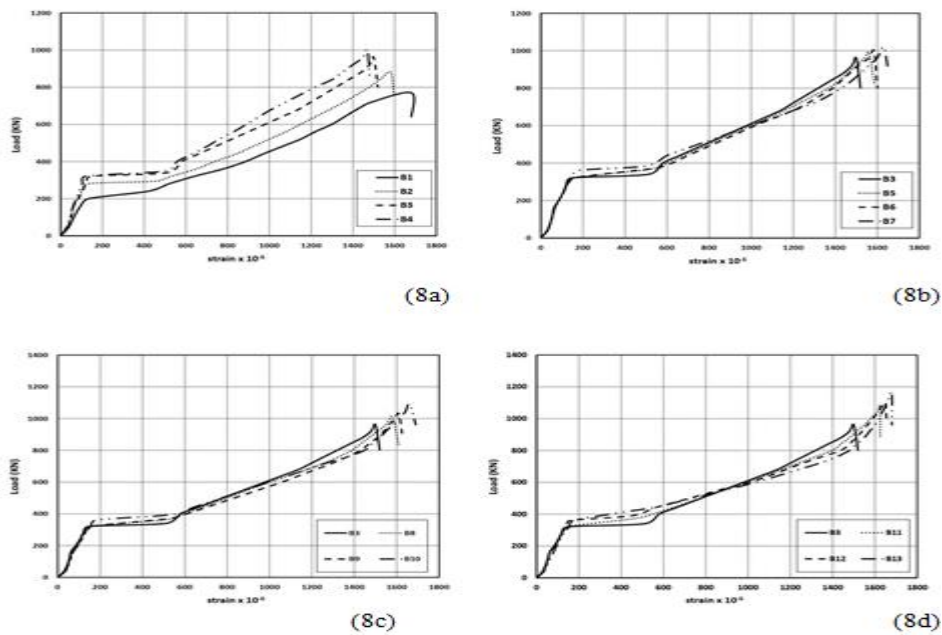
3.5. Strains in vertical and horizontal stirrups
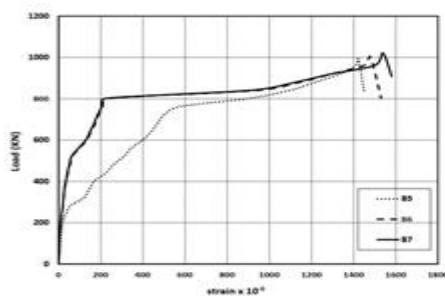
The strain in vertical and horizontal stirrups was plotted, as shown in Fig. 9 and Fig. 10. Shear stirrups began to pick up strains once the inclined cracks occurred, indicating that the vertical and horizontal stirrups both contributed to shear resistance. Measurements of strain in stirrups showed that the transverse reinforcement yielded before the specimen broke reached the strain hardening range with strains much higher than the yield strain. This means that the vertical and horizontal stirrups were able to resist shear stresses in deep beams.

(8a)   (8b)

(8c)   (8d)

Fig 8. Load-strain curve in bottom bars

Fig 9.Load-strain curve in vertical stirrups   **Fig10**. Load-strain curve in horizontal stirrups
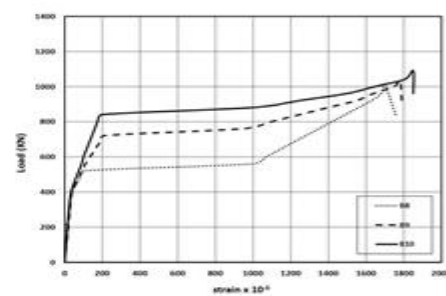
4. THE EFFECT OF STUDY PARAMETERS
4.1. Polypropylene fiber content

The impact of polypropylene fiber content on the behavior of SCC deep beams was determined by testing four specimens. The test results demonstrate that the cracking and ultimate load-carrying capacity of SCC deep beams have improved significantly. As shown in Table 5, the cracking load increased by 25%, 42%, and 47% for specimens B2, B3, and B4, and the ultimate load

increased by 14%, 25%, and 30% for specimens B2, B3, and B4, respectively, compared to specimen B1, containing no shear reinforcement. In addition, raising the percentage of polypropylene fibers from 0% to 0.90 % raised the ultimate displacement to around 45 %. The estimated absorbed energy validates the enhanced performance of the polypropylene fiber-reinforced specimens. The greatest increase in energy absorption was roughly 108%. Polypropylene fibers increase the biaxial strength of SCC deep beams, which improves their resistance to cracking and ultimate load-bearing capability, in the absence of shear reinforcement.

4.2. Vertical shear reinforcement

To avoid strut splitting failure, ACI 318 [1] recommends providing minimum shear reinforcement in both vertical and horizontal directions. The influence of vertical stirrups alone on the behavior of SCC deep beams was determined by testing three beams. Fiber content was 0.6 % in all specimens. Clearly, the use of vertical stirrups decreases deflection and increases the ultimate capacity of specimens B5, B6, and B7, as shown in Fig. 6b. As the number of stirrups increases and their distance decreases, the deflection slightly decreases. In comparison with the control Specimen B3, the cracking load increased by about 8%, 11%, and 13% for B5, B6, and B7, respectively. The maximum increase in the ultimate load, on the other hand, was about 6.25 %. The absorbed energy increased by about 14.5%, 27%, and 39% for B5, B6, and B7.

4.3. Horizontal shear reinforcement

Both vertical and horizontal web reinforcements are effective for enhancing the shear capacity of deep beams. three specimens evaluated the influence of horizontal web reinforcement on deep beam performance. the cracking load increased by about 8%, 9%, and 17% for B8, B9, and B10, respectively, as shown in Fig. 6c. The maximum increase in the ultimate load, on the other hand, was about 14%. The horizontal and vertical web reinforcements were obviously similarly efficient in providing shear strength to the tested beams. The absorbed energy increased by about 13%, 24.5%, and 49% for B8, B9, and B10.

5. PREDICTION OF THE DEEP BEAM BASED ON EQUATIONS
5.1. Kong et al. (1978)

Kong et al. [30] conduct an experiment to predict the ultimate shear strength of a solid deep beam. Equations for calculating the ultimate shear strength of a solid deep beam

are offered. Using Eq .(1), the web reinforcement ratio of solid beams with varying web reinforcement ratios is determined.

$$V_n = Q_{ult} = C1 \left[1 - 0.35 \frac{X}{D} \right] f_t b D + C2 \sum A \frac{y}{D} \sin^2 \alpha \quad (1)$$

Where $C1$ is an empirical coefficient ($C1 = 1.40$ for normal weight concrete); C 2 is an empirical coefficient ($C2 = 300$ N / mm ^{2} for deformed bars, and 130 N / mm ^{2} for plain round bars); D is the overall depth of the deep beam; f_t is the concrete's cylinder splitting tensile strength ($0.6 \sqrt{f_{cu}}$ N/mm ^{2}); y depth at which a typical bar intersects a potential critical diagonal crack; α angle of intersection between a typical bar and a potential critical diagonal crack; b is the width of the deep beam; f_{cu} Cube strength of concrete; A area of a web bar and longitudinal bars. Table 6 presents the expected result for ultimate shear capacity, which was determined by updating the equation used by Kong et al. to provide the best estimate for specimens examined with and without web reinforcement. Furthermore, the modified equation is as follows:

$$V_n = \frac{1}{10} \left[1 - 0.35 \frac{X}{D} \right] f_c' b D + C2 \sum A \frac{y}{D} \sin^2 \alpha \quad (2)$$

5.2. ACI 318-19 STM model
The following formula is used to represent the strut's nominal compressive strength F_{ns} according to ACI 318-19:
$$F_{ns} = f_{ce} A_{cs} \quad (3)$$

Where: A_{cs} is the cross-sectional area of the strut, and f_{ce} is the concrete's effective compressive strength.
$$f_{ce} = 0.85 \beta_c \beta_s f_c' \quad (4)$$

Where: β_s, β_c; is defined by ACI 318-19. Tables 23.4.3(a) and 23.4.3(b), respectively. The effective concrete strength under compression force is represented by the coefficient $0.85 f_c'$.
The nominal tension strength of the tie F_{nt} is given by the formula:
$$F_{nt} = f_y A_{ts} \quad (5)$$

The nominal compressive strength of the nodal zone, F_{nn}, is calculated by:
$$F_{nn} = f_{ce} A_{nz} \quad (6)$$
$$f_{ce} = 0.85 \beta_c \beta_n f_c' \quad (7)$$

Where: β_n, β_c; is defined by ACI 318-19. Tables 23.9.2 and 23.4.3(b), respectively.

6. COMPARISON OF PREDICTED AND EXPERIMENTAL RESULTS

Table 6 displays the calculated ultimate shear strengths for the tested beams with various web reinforcement ratios

based on the models and equations stated in the preceding section. The predicted ultimate strength of deep beams using ACI 318-19 is quite conservative. The excessive conservatism necessitated the introduction of new phrases.

The updated equation created by the authors and produced by Kong et al. based shear strength prediction produced the most accurate assessment of ultimate shear capacity for deep beams with various web reinforcement ratios.

Table 6. Prediction of ultimate shear strength

Beam No.	Δ_{cr} (mm)	P_{cr} (KN)	Δ_u (mm)	P_u (KN)	Absorbed energy (KN.mm)	Failure mode
B1	1.20	240	3.60	770	1411	Shear splitting
B2	1.56	300	4.50	880	2231	Shear splitting
B3	1.69	340	4.90	960	2618	Shear splitting
B4	1.79	352	5.22	1000	2939	Shear splitting
B5	1.80	368	5.25	990	2998	Shear splitting
B6	1.85	376	5.60	1000	3333	Shear crushing
B7	1.92	385	5.92	1020	3637	Shear crushing
B8	1.76	365	5.18	1009	2949	Shear crushing
B9	1.82	370	5.50	1030	3259	Shear splitting
B10	1.95	396	6.00	1090	3900	Shear crushing
B11	2.00	375	6.12	1080	3816	Shear crushing
B12	2.10	390	6.30	1100	4074	Shear crushing
B13	2.22	415	6.54	1165	4481	Shear crushing

7. CONCLUSION

The main conclusions of the current investigation could be stated as follows:

- As anticipated, the failure mode for all tested SCC deep beams was a shear failure.
- The insertion of polypropylene fibers enhanced the cracking load, ultimate capacity, displacement, and energy absorption of SCC deep beams with no web reinforcement that were put to the test. Based on the range of examined values, a 0.9% polypropylene fiber content led to the largest improvement in beam performance with no web reinforcement. The ultimate capacity and displacement increased by approximately 30% and 45%, respectively. The increase in energy absorption capacity was around 108%.
- Addition of horizontal web reinforcement to the beam containing polypropylene fibers resulted in an increase of 13.5 % in the ultimate load capacity and an increase of 22.4 % in ultimate displacement.

- Addition of vertical web reinforcement to the beam containing polypropylene fibers resulted in an increase of 6.25 % in the ultimate load capacity and an increase of 21 % in ultimate displacement.
- As vertical and horizontal web reinforcement increased, the tested deep beam's energy absorption increased.
- Comparing the experimental shear strengths to the predicted values using the available equations, the modified equation for Kong et al. based shear strength methods generated the most accurate results.

Shear splitting failure was observed in SCC deep beams without horizontal stirrups, but shear crushing failure was observed in the same beams with horizontal web reinforcement

REFERENCES

[1]　　ACI 318-19, Building code requirements for structural concrete (ACI 318-19) : an ACI standard ; Commentary on building code

requirements for structural concrete (ACI 318R-19), American Concrete Institute, Farmington Hills MI, 2019.

[2] G. Russo, R. Venir, M. Pauletta, Reinforced concrete deep beams-shear strength model and design formula, ACI Struct J. 102 (2005) 429.

[3] M.A. Adam, M. Said, T.M. Elrakib, Shear performance of fiber reinforced self-compacting concrete deep beams, Int. J. Civ. Eng. Technol.(IJCIET). 7 (2016) 25–46.

[4] A. Ismail el-kassas, H.M. Hassan, M.A.E.S. Arab, Effect of longitudinal opening on the structural behavior of reinforced high-strength self-compacted concrete deep beams, Case Studies in Construction Materials. 12 (2020).

[5] A.C.I.C. 237, Self-consolidating concrete, in: American Concrete Institute, 2007.

[6] C. Parra, M. Valcuende, F. Gómez, Splitting tensile strength and modulus of elasticity of self-compacting concrete, Constr Build Mater. 25 (2011) 201–207.

[7] D. Karthik, K. Nirmalkumar, R. Priyadharshini, Characteristic assessment of self-compacting concrete with supplementary cementitious materials, Constr Build Mater. 297 (2021) 123845.

[8] H. Okamura, S.H.P. Concrete, Social System Institute, (1999).

[9] K.S. Mahmoud, Experimental study of the shear behavior of self compacted concrete T-beams, Journal of Engineering and Development. 16 (2012).

[10] A.A.A. Hassan, K.M.A. Hossain, M. Lachemi, Structural assessment of corroded self-consolidating concrete beams, Eng Struct. 32 (2010) 874–885.

[11] M. Lachemi, K.M.A. Hossain, V. Lambros, P.-C. Nkinamubanzi, N. Bouzoubaâ, Self-consolidating concrete incorporating
new viscosity modifying admixtures, Cem Concr Res. 34 (2004) 917–926.

[12] Y. Choulli, A.R. Marí, A. Cladera, Shear behaviour of full-scale prestressed i-beams made with self compacting concrete, Materials and Structures/Materiaux et Constructions. 41 (2008) 131–141.

[13] A.A. Zende, R.B. Khadiranaikar, A.Iqbal.A. Momin, Shear behaviour of high strength self-compacting concrete with varying stirrup spacing, International Journal of Structural Engineering. 12 (2022) 374.

[14] R. Narayan, I.Y.S. Darwish, Fiber concrete deep beams in shear, Structural Journal. 85 (1988) 141–149.

[15] M.A. Mansur, K.C.G. Ong, Behavior of reinforced fiber concrete deep beams in shear, Structural Journal. 88 (1991) 98–105.

[16] V. Afroughsabet, T. Ozbakkaloglu, Mechanical and durability properties of high-strength concrete containing steel and polypropylene fibers, Constr Build Mater. 94 (2015) 73–82.

[17] L. Xu, C. Wei, B. Li, Damage Evolution of Steel-Polypropylene Hybrid Fiber Reinforced Concrete: Experimental and Numerical Investigation, Advances in Materials Science and Engineering. 2018 (2018).

[18] P. Zhang, Q. Li, Z. Sun, Effect of polypropylene fibre on flexural properties of concrete composites containing fly ash and silica fume, Proceedings of the Institution of Mechanical Engineers,
Part L: Journal of Materials: Design and Applications. 226 (2012) 177–181.

[19] P. Zhang, Q. Li, Fracture properties of polypropylene fiber reinforced concrete containing fly ash and silica fume, Research Journal of Applied Sciences, Engineering and Technology. 5 (2013) 665–670.

[20] S. Khan, R.A. Khan, A.R. Khan, M. Islam, S. Nayal, Mechanical properties of Polypropylene Fibre reinforced concrete for M 25 & M 30 mixes: A Comparative study,

International Journal of Scientific Engineering and Applied Sciences. 1 (2015).

[21] D.S. Dharan, A. Lal, Study the effect of polypropylene fiber in concrete, International Research Journal of Engineering and Technology. 3 (2016) 616–619.

[22] S.U. Hong, Y.T. Lee, S.H. Kim, S.K. Baek, Y.S. Cho, Strength properties of recycled aggregate concrete mixed with polypropylene fiber, in: Applied Mechanics and Materials, Trans Tech Publ, 2012: pp. 28–31.

[23] W.N.S.W. Mohammad, S. Ismail, W.A.W. Alwi, Properties of recycled aggregate concrete reinforced with polypropylene fibre, in: MATEC Web of Conferences, EDP Sciences, 2016: p. 77.

[24] B.M. Hanumesh, B.A. Harish, N.V. Ramana, Influence of polypropylene fibres on recycled aggregate concrete, Mater Today Proc. 5 (2018) 1147–1155.

[25] Z. Yuan, Y. Jia, Mechanical properties and microstructure of glass fiber and polypropylene fiber reinforced concrete: An experimental study, Constr Build Mater. 266 (2021).

[26] S. Elkatatny, R. Gajbhiye, A. Ahmed, A.A. Mahmoud, Enhancing the cement quality using polypropylene fiber, J Pet Explor Prod Technol. 10 (2020) 1097–1107.

[27] A.C. Institute, State-of-the-art report on high-strength concrete, American Concrete Institute, Farmington Hills, Michigan. (1992).

[28] M. Mohammadhassani, M.Z. Jumaat, A. Ashour, M. Jameel, Failure modes and serviceability of high strength self compacting concrete deep beams, Eng Fail Anal. 18 (2011) 2272–2281.

[29] I.G. Shaaban, A.H. Zaher, M. Said, W. Montaser, M. Ramadan, G.N. Abd Elhameed, Effect of partial replacement of coarse aggregate by polystyrene balls on the shear behaviour of deep beams with web openings, Case Studies in Construction Materials. 12 (2020).

[30] F.K. Kong, G.R. Sharp, S.C. Appleton, C.J. Beaumont, L.A. Kubik, Structural idealization for deep beams with web openings: further evidence, Magazine of Concrete Research. 30 (1978) 89–95.